Contribution from the Department of Chemistry,
University of California, Berkeley, California 94720

Zinc, Cadmium, and Mercury Tellurolates: Hydrocarbon Solubility and Low Coordination Numbers Enforced by Sterically Encumbered Silyltellurolate Ligands

Philip J. Bonasia and John Arnold*

Received March 5, 1992

We describe the preparation of homoleptic zinc, cadmium, and mercury tellurolates incorporating the bulky sitel anion [sitel = $^-TeSi(SiMe_3)_3$] and their characterization by ^1H, ^{31}P, ^{113}Cd, ^{199}Hg, and ^{125}Te NMR spectroscopy and X-ray crystallography. All three derivatives $M[TeSi(SiMe_3)_3]_2$ (**1**, M = Zn; **2**, M = Cd; **3**, M = Hg) are prepared via tellurolysis of $M[N(SiMe_3)_2]_2$ with $HTeSi(SiMe_3)_3$ or, for **3**, by reaction of Li(sitel) with $HgCl_2$. The zinc and cadmium compounds exist as dimers in solution, with two bridging and two terminal tellurolate ligands; these exchange rapidly on the NMR time scale at room temperature. Below −30 °C, this process is frozen out as evidenced by ^1H, ^{113}Cd, and ^{125}Te NMR spectroscopy. In contrast, ^1H and $^{125}Te\{^1H\}$ NMR studies show **3** to be monomeric in solution. Vapor pressure molecular weight measurements in benzene indicate molecular weights higher than those expected for monomeric species, with the tendency toward dimerization increasing in the order Cd > Zn > Hg. The dimeric nature of **1** in the solid state has been determined by X-ray crystallography; it crystallizes from hexane in the space group $P\bar{1}$ with a = 14.804 (5) Å, b = 16.458 (5) Å, c = 18.237 (5) Å, α = 63.97 (2)°, β = 84.61 (2)°, γ = 79.47 (2)°, V = 3925 (2) Å^3, d_{calcd} = 1.38 g cm^{-3}, and Z = 2. Reaction of **1** with 2 equiv of pyridine affords the monomeric zinc tellurolate $Zn[TeSi(SiMe_3)_3]_2(pyr)_2$ (**4**), while reaction with bipyridine (bpy) produces the related adduct $Zn[TeSi(SiMe_3)_3]_2(bpy)$ (**5**). Compound **4** crystallizes from dichloromethane in the space group $P\bar{1}$ with a = 11.919 (2) Å, b = 12.1397 (2) Å, c = 17.319 (3) Å, α = 105.33 (1)°, β = 99.71 (2)°, γ = 96.28 (1)°, V = 2350 (2) Å^3, d_{calcd} = 1.38 g cm^{-3}, and Z = 2. Similarly, monomeric cadmium tellurolates are formed by reaction of **2** with either bpy or dmpe [dmpe = 1,2-bis(dimethylphosphino)ethane] to give $Cd[TeSi(SiMe_3)_3]_2(bpy)_2$ (**6**) and $Cd[TeSi(SiMe_3)_3]_2(dmpe)$ (**7**). The dmpe adduct **7** crystallizes in the space group $P2_12_12_1$ with a = 13.149 (2) Å, b = 25.552 (3) Å, c = 28.535 (4) Å, V = 9588 (2) Å^3, d_{calcd} = 1.40 g cm^{-3}, and Z = 8.

Introduction

In general, the chemistry of group 12 metal chalcogenolates is complicated by the formation of oligomeric networks supported by bridging chalcogenolate ligands, as exemplified by such compounds as the polyadamantoid $[Cd(SPh)_2]_n$.[1-3] This is especially true for ligands based on the lighter chalcogens, but for tellurium the situation is less clear, since its chemistry is poorly understood. Most work to date has centered on phenyltellurolates where structures of the simplest, homoleptic derivatives are presumed to involve coordination polymers, such as $[Hg(TePh)_2]_n$.[4,5] Manipulation of aryl substituents in order to tailor desirable physical properties, such as lower molecularity and enhanced solubilities, is a well-proven tactic in the chemistry of related alkoxides and thiolates.[6-9] Efforts to extend this strategy to tellurolate chemistry have resulted in the preparation of various ortho-substituted aryltellurolates with mesityl, triisopropylphenyl, or tri-*tert*-butylphenyl,[10,11] and examples of some of their group 12 derivatives have been reported.[12,13] As these studies have shown, however, incorporation of bulky aryl substituents does not necessarily ensure that stable, low-molecularity complexes will result. For example, mesityl substituents are not sufficiently bulky to prevent polymerization, as revealed by the X-ray structure of the cadmium mesityl derivative $\{Cd[Te(2,4,6\text{-}Me_3C_6H_2)]_2\}_m$ which shows it to be polymeric with bridging tellurolates.[14] The mercury analogue $\{Hg[Te(2,4,6\text{-}Me_3C_6H_2)]_2\}_n$ is relatively insoluble in hydrocarbons, and the corresponding triisopropylphenyl complex is thermally unstable.[13]

Much of the recent interest in this general class of compounds has been directed toward their use as single-source precursors to binary II/VI semiconductors, such as CdS,[15,16] CdSe,[12,16] CdTe,[17] and HgTe.[18] Bulk and nanocluster-sized samples have been prepared from these molecules; however, efforts to prepare thin films of II/VI materials via chemical vapor deposition (CVD) are hindered by the low thermal stabilities and low volatilities of the precursors.

We have been developing tellurolate chemistry incorporating the very bulky sitel ligand (sitel = $^-TeSi(SiMe_3)_3$), and our recent results demonstrate that this ligand forms stable complexes with a wide variety of metals.[19] This paper focuses on the synthesis and structure of low-coordinate homoleptic zinc, cadmium, and mercury sitel derivatives, whose physical and chemical properties differ considerably from those of previously reported group 12 tellurolates. Included are the first examples of zinc tellurolates, X-ray crystal structures of two derivatives, and the first monomeric cadmium tellurolate. We also describe detailed ^{125}Te NMR studies which serve to characterize the solution behavior of these compounds. Details of CVD experiments using these compounds as precursors to II/VI thin films will be reported later.[20]

Experimental Section

Our standard operating procedures were as described previously.[21] 2,2'-Bipyridyl (bpy) was recrystallized from ethanol, dmpe[22] was purified by distillation under vacuum, and 4-*tert*-butylpyridine (Aldrich) was used as received. The metal amides were prepared as described by Bürger.[23] Vaporimetric molecular weight measurements (conducted in duplicate

(1) Craig, D.; Dance, I. G.; Garbutt, R. *Angew. Chem., Int. Ed. Engl.* **1986**, *25*, 165.
(2) Dance, I. G. *Polyhedron* **1986**, *5*, 1037.
(3) Gysling, H. J. In *The Chemistry of Organic Selenium and Tellurium Compounds*; Patai, S., Rappoport, Z., Eds.; Wiley: New York, 1986; Vol. 1, p 679.
(4) Gysling, H. J. *Coord. Chem. Rev.* **1982**, *42*, 133.
(5) Okamoto, Y.; Yano, T. *J. Organomet. Chem.* **1971**, *29*, 99.
(6) For reviews, see: Bradley, D. C.; Mehrotra, R. C.; Gaur, D. P. *Metal Alkoxides*; Academic: New York, 1978. Mehrotra, R. C. *Adv. Inorg. Chem. Radiochem.* **1983**, *26*, 269. Rothwell, I. P. R.; Chisholm, M. H. In *Comprehensive Coordination Chemistry*; Wilkinson, G., Gillard, R. D., McCleverty, J. A., Eds.; Pergamon: New York, 1987; Vol. 2, p 335.
(7) Horvath, B.; Möseler, R.; Horvath, E. G. *Z. Anorg. Allg. Chem.* **1979**, *449*, 41.
(8) Bartlett, R. A.; Ellison, J. J.; Power, P. P.; Shoner, S. C. *Inorg. Chem.* **1991**, *30*, 2888.
(9) Santos, R. A.; Gruff, E. S.; Koch, S. A.; Harbison, G. S. *J. Am. Chem. Soc.* **1991**, *113*, 469.
(10) Lange, L.; Du Mont, W. W. *J. Organomet. Chem.* **1985**, *286*, C1.
(11) Bonasia, P. J.; Arnold, J. *J. Chem. Soc., Chem. Commun.* **1990**, 1299.
(12) Brennan, J. G.; Siegrist, T.; Carroll, P. J.; Stuczynski, S. M.; Reynders, P.; Brus, L. E.; Steigerwald, M. L. *Chem. Mater.* **1990**, *2*, 403.
(13) Bochmann, M.; Webb, K. J. *J. Chem. Soc., Dalton Trans.* **1991**, 2325.
(14) Bochmann, M.; Coleman, A. P.; Webb, K. J.; Hursthouse, M. B.; Mazid, M. *Angew. Chem., Int. Ed. Engl.* **1991**, *30*, 973.
(15) Brennan, J. G.; Siegrist, T.; Carroll, P. J.; Stuczynski, S. M.; Brus, L. E.; Steigerwald, M. L. *J. Am. Chem. Soc.* **1989**, *111*, 4141.
(16) Bochmann, M.; Webb, K.; Harman, M.; Hursthouse, M. B. *Angew. Chem., Int. Ed. Engl.* **1990**, *29*, 638.
(17) Steigerwald, M. L.; Sprinkle, C. R. *J. Am. Chem. Soc.* **1987**, *109*, 7200.
(18) Steigerwald, M. L.; Sprinkle, C. R. *Organometallics* **1988**, *7*, 245.
(19) Dabbousi, B. O.; Bonasia, P. J.; Arnold, J. *J. Am. Chem. Soc.* **1991**, *113*, 3186.
(20) Bonasia, P. J.; Seligson, A.; Arnold, J.; Walker, J.; Bourret, E. D. Submitted for publication.
(21) Bonasia, P. J.; Gindelberger, D. E.; Dabbousi, B. D.; Arnold, J. *J. Am. Chem. Soc.*, in press.
(22) Burt, R. J.; Chatt, J.; Hussian, W.; Leigh, G. J. *J. Organomet. Chem.* **1979**, *182*, 203.
(23) Bürger, H.; Sawodny, W.; Wannagat, U. *J. Organomet. Chem.* **1965**, *3*, 113.

0020-1669/92/1331-2508$03.00/0

for each sample analyzed) were determined in benzene under nitrogen by Pascher, Remagen, Germany.

NMR Studies. Proton NMR spectra were recorded in benzene-d_6 at 20 °C unless stated otherwise. $^{31}P\{^1H\}$ NMR spectra were recorded at 161.977 MHz, with chemical shifts relative to external 85% H_3PO_4 at 0 ppm. $^{125}Te\{^1H\}$, $^{113}Cd\{^1H\}$, and $^{199}Hg\{^1H\}$ NMR samples were prepared in 5-mm NMR tubes sealed with rubber septa under dinitrogen. The spectra were recorded at ambient temperatures, unless stated otherwise, on a Bruker AM-500 NMR spectrometer equipped with a 5-mm dual proton broad-band probe (from 15 to 203 MHz) at 157.905, 110.937, and 89.578 MHz, respectively. The $^{125}Te\{^1H\}$ spectra were indirectly referenced to neat Me_2Te at 0 ppm[24-26] by direct reference to external $Te(OH)_6$ (1.74 M in D_2O, 20 °C) at 712 ppm;[24,27] these data are recorded in Table II. $^{113}Cd\{^1H\}$ data were relative to $Cd[ClO_4]_2$ at 0 ppm by direct reference to $CdBr_2$ (1.0 M in D_2O, 20 °C) at 109 ppm;[26] $^{199}Hg\{^1H\}$ chemical shifts were relative to $HgMe_2$ at 0 ppm by direct reference to Ph_2Hg (1.0 M in CH_2Cl_2, 20 °C) at −745 ppm.[26]

Preparation of Compounds. $\{Zn[TeSi(SiMe_3)_3]_2\}_2$ (1). A solution of 0.32 g (0.83 mmol) of $Zn[N(SiMe_3)_2]_2$ in 25 mL of hexane was added to a solution of 0.625 g (1.66 mmol) of $HTeSi(SiMe_3)_3$ in 25 mL of the same solvent, resulting in the immediate formation of a yellow solution. This mixture was stirred for 30 min, and the solvent was removed under reduced pressure. The dry yellow solid was extracted with hexamethyldisiloxane (40 mL); then the solution was filtered, concentrated to 15 mL, and cooled to −40 °C for 12 h. Clear yellow cubes (0.504 g, 74%) of the product were isolated by filtration. Mp: 208–213 °C. ^1H NMR (300 MHz): δ 0.45 (s). IR: 1397 s, 1277 w, 1258 s, 1244 s, 1174 w, 1034 w, 840 s, 744 m, 734 m, 689 s, 645 w, 638 w, 623 s, 462 w, 455 w, 400 w, 390 w, 303 m, 297 m cm^{-1}. MS (EI, 70 eV): m/z 816 (M^+), 551, 478, 73. Molecular weight (vaporimetric): 913, 914. Anal. Calcd for $C_{18}H_{54}Si_8Te_2Zn$: C, 26.5; H, 6.67. Found: C, 26.6; H, 6.87.

$\{Cd[TeSi(SiMe_3)_3]_2\}_2$ (2). $Cd[N(SiMe_3)_2]_2$ (0.609 g, 1.41 mmol) dissolved in 25 mL of hexane was combined with 1.06 g (2.82 mmol) of $HTeSi(SiMe_3)_3$ dissolved in 25 mL of hexane. Workup as above, followed by crystallization from hexane (15 mL) at −40 °C, gave a yellow powder (0.845 g, 69%). Mp: 210–220 °C. ^1H NMR (300 MHz): δ 0.43 (s). $^{113}Cd\{^1H\}$ NMR (toluene-d_8, −75 °C, 0.18 M): δ 117 (s, $|J_{^{113}Cd^{125}Te}|$ = 1088 Hz, $|J_{^{113}Cd^{123}Te}|$ = 1904 Hz). IR: 1397 s, 1244 s, 1096 w, 1066 w, 1029 w, 838 s, 746 m, 691 s, 623 s, 457 w, 396 m cm^{-1}. MS (EI, 70 eV): m/z 863 (M^+), 551, 478, 405, 73. Molecular weight (vaporimetric): 1095, 1130. Anal. Calcd for $C_{18}H_{54}Si_8Te_2Cd$: C, 25.1; H, 6.31. Found: C, 25.2; H, 6.34.

$Hg[TeSi(SiMe_3)_3]_2$ (3). Method A. The compound was prepared as for **1** and **2**. $Hg[N(SiMe_3)_2]_2$ (0.50 g, 1.0 mmol) in 25 mL of hexane was combined with $HTeSi(SiMe_3)_3$ (0.75 g, 2.0 mmol) in 30 mL of hexane to give a yellow-brown solution. After 30 min of stirring, no further darkening was observed and the solvent was removed under reduced pressure. Extraction with hexamethyldisiloxane (45 mL) gave a yellow solution, which was filtered, concentrated, and cooled to −40 °C. After 24 h, filtration afforded the product as transparent green crystals (0.778 g, 82%).

Method B. Diethyl ether (70 mL) was added to a stirred mixture of 1.25 g (2.4 mmol) of $(THF)_2LiTeSi(SiMe_3)_3$ and 0.33 g (1.20 mmol) of $HgCl_2$. The brown mixture was stirred for 12 h, after which no further darkening was observed. The solvent was removed under reduced pressure, and the residue was extracted with pentane (50 mL). The yellow solution was filtered, concentrated to 10 mL, and cooled to −40 °C. After 12 h, 0.763 g (67%) of clear green-yellow crystals were isolated by filtration. Mp: 166–172 °C. ^1H NMR (300 MHz): δ 0.32 (s). $^{199}Hg\{^1H\}$ NMR (toluene-d_8, 26 °C, 0.21 M): δ −2328 (s). IR: 1394 s, 1256 s, 1241 s, 1097 m, 1031 w, 834 s, 744 s, 688 s, 622 s, 459 w cm^{-1}. MS (EI, 70 eV): m/z 951 (M^+), 551, 478, 73. Molecular weight (vaporimetric): 896, 906. Anal. Calcd for $C_{18}H_{54}Si_8Te_2Hg$: C, 22.7; H, 5.72. Found: C, 22.5; H, 5.87.

$Zn[TeSi(SiMe_3)_3]_2(pyr)_2$ (4). Via syringe, pyridine (66 μL, 0.80 mmol) was added to a solution of **1** (0.33 g, 0.40 mmol) in hexane (30 mL). The clear yellow solution quickly turned lighter as a pale yellow microcrystalline solid precipitated. Volatile components were removed under reduced pressure, and the material was extracted with dichloromethane (25 mL). The clear yellow solution was filtered, concentrated to 10 mL, and cooled to −40 °C. After 24 h, clear yellow cubes were observed floating in the dichloromethane. Filtration afforded the product in 90% yield (0.350 g). The crystals lose pyridine at 90 °C and then slowly decompose to a dark red-orange material above 151 °C. ^1H NMR ($CDCl_3$, 400 MHz): δ 9.00 (m, 4 H), 7.79 (m, 2 H), 7.38 (m, 4 H), 0.14 (s, 54 H). IR: 3069 m, 1602 s, 1573 w, 1487 s, 1448 s, 1396 m, 1357 m, 1254 m, 1241 s, 1217 m, 1153 m, 1069 s, 1037 s, 1010 s, 866 s, 750 s, 738 m, 723 m, 696 s, 689 s, 669 m, 630 s, 622 s, 423 m, 419 m, 408 m cm^{-1}. MS (EI, 70 eV): m/z 816 (M^+ − 2pyr) 624, 551, 79, 73. Anal. Calcd for $C_{28}H_{64}N_2Si_8Te_2Zn$: C, 34.5; H, 6.62; N, 2.88. Found: C, 34.4; H, 6.60; N, 2.63.

$Zn[TeSi(SiMe_3)_3]_2(bpy)$ (5). A solution of bpy (0.06 g, 0.39 mmol) in 30 mL of toluene was added to a solution of **1** (0.30 g, 0.36 mmol) in 30 mL of toluene, resulting in an immediate color change to orange-red and precipitation of a fine orange material. The toluene was removed under reduced pressure, and the light orange product was extracted with dichloromethane. The resulting dark red solution was filtered, concentrated from 75 to 45 mL, and allowed to cool to 0 °C overnight. Thin orange needles (0.276 g, 71%) were isolated by filtration. The material was also obtained as dark red diamond-shaped plates by more slowly cooling an analogous solution to 0 °C over a period of 24 h. The material melts to a red-black liquid between 260 and 270 °C. ^1H NMR (CD_2Cl_2, 500 MHz): δ 9.00 (m, 2 H), 8.24 (m, 2 H), 8.12 (m, 2 H), 7.68 (m, 2 H), 0.01 (s, 54 H). IR: 1603 m, 1596 s, 1564 w, 1489 m, 1442 s, 1313 m, 1256 m, 1241 s, 1155 m, 1023 m, 1012 m, 861 s, 836 s, 772 s, 736 m, 689 s, 632 m, 621 s cm^{-1}. MS (EI, 70 eV): m/z 816 (M^+ − bpy), 551, 478, 73. Anal. Calcd for $C_{28}H_{62}Si_8N_2Te_2Zn$: C, 34.6; H, 6.43; N, 2.88. Found: C, 34.8; H, 6.19; N, 2.75.

$Cd[TeSi(SiMe_3)_3]_2(bpy)$ (6). A toluene solution of bipyridine (0.047 g, 0.30 mmol in 10 mL) was added to a solution of **2** (0.30 g, 0.35 mmol) in the same solvent (25 mL). After being stirred for several minutes, the clear red solution became orange-yellow and a fine yellow powder precipitated. The toluene was removed under reduced pressure, and the residue was extracted with dichloromethane (40 mL). The dark orange-red solution was filtered, concentrated to 15 mL, and cooled to −40 °C for 12 h. Thin yellow needles of the product were collected by filtration (0.233 g, 76%). Mp: 241–243 °C. ^1H NMR (CD_2Cl_2, 500 MHz): δ 8.86 (m, 2 H), 8.20 (m, 2 H), 8.05 (m, 2 H), 7.60 (m, 2 H), 0.10 (s, 54 H). IR: 1597 m, 1488 m, 1439 s, 1311 m, 1257 m, 1240 s, 1100 w, 1061 w, 1015 m, 861 s, 836 s, 767 m, 688 m, 648 w, 622 m, 420 w, 412 w, 403 w cm^{-1} MS (EI, 70 eV): m/z 863 (M^+ − bpy), 551, 478, 73. Anal. Calcd for $C_{28}H_{62}Si_8N_2Te_2Cd$: C, 33.0; H, 6.13; N, 2.75. Found: C, 32.8; H, 5.88; N, 2.48.

$Cd[TeSi(SiMe_3)_3]_2(dmpe)$ (7). Via syringe, dmpe (79 μL, 0.47 mmol) was added to a solution of **2** (0.404 g, 0.468 mmol) in 50 mL of hexane. After being stirred for several minutes, the yellow solution became cloudy and pale yellow needles precipitated. The hexane was removed under reduced pressure, and the residue was extracted with dichloromethane (40 mL). The filtrate was concentrated to 10 mL and cooled to −40 °C for 24 h to afford the product (0.365 g, 77%) as large clear yellow crystals. The crystals lose dmpe by 200 °C and slowly decompose from 280 to 300 °C. ^1H NMR (300 MHz): δ 0.98 (m, 4 H), 0.88 (br s, 12 H), 0.49 (s, 54 H). $^{31}P\{^1H\}$ NMR (CD_2Cl_2, −90 °C, 0.11 M): δ −40.8 (s, $|^2J_{^{P125}Te}|$ = 140 Hz, $|^2J_{^{P123}Te}|$ 114 Hz, $|J_{^{P113}Cd}|$ = 251 Hz, $|J_{^{P111}Cd}|$ = 240 Hz. $^{113}Cd\{^1H\}$ NMR (CD_2Cl_2, −71 °C, 0.10 M): δ 426 (s, $|J_{^{113}CdTe}|$ = 711 Hz, $|J_{^{113}CdP}|$ = 233 Hz). IR: 1424 m, 1419 m, 1302 w, 1284 w, 1253 m, 1240 s, 1137 w, 948 s, 928 m, 889 m, 858 s, 835 s, 739 m, 703 m, 687 s, 643 w, 623 s, 406 m cm^{-1}. MS (EI, 70 eV): m/z 910, 782, 579, 450. Anal. Calcd for $C_{24}H_{70}Si_8Te_2P_2Cd$: C, 28.5; H, 6.96. Found: C, 28.3; H, 6.98.

X-ray Structural Studies. The accurate cell dimensions and their esd's for **1**, **4**, and **7** were derived by a least-squares fit to the setting angles of the unresolved Kα components of 24 reflections with 2θ between 26 and 32° for **1** and between 20 and 26° for **4** and **7**. Intensity standards were measured on the diffractometer using graphite-monochromated Mo Kα radiation every 1 h of data collection. Intensity standards for **1**, **4**, and **7** over the data collection period, showed 4.1%, 3.5%, and 4.3% decreases, respectively. For each compound, three reflections were checked after every 200 measurements as orientation checks. Crystal orientation was redetermined if any of the reflections were offset by more than 0.01° from their predicted positions; such reorientations were not necessary during data collection for any compound. Linear corrections for decay and appropriate absorption corrections were made for each of the compounds.

The crystal structures for **1** and **7** were solved by direct methods using the SHELXS-86 program,[28] while Patterson–Fourier methods were used to determine the structure of **4**. For each compound, the positional and

(24) McFarlane, H. C. E.; McFarlane, W. In *Multinuclear NMR*; Mason, J., Ed.; Plenum Press: New York, 1987; Vol. 1, p 417.
(25) Luthra, N. P.; Odom, J. E. In *The Chemistry of Organic Selenium and Tellurium Compounds*; Patai, S., Ed.; John Wiley & Sons Ltd.: New York, 1986; Vol. 1, p 189.
(26) Rodger, C.; Sheppard, N.; McFarlane, H. C. E.; McFarlane, W. In *NMR and the Periodic Table*; Harris, R. K., Mann, B. E., Eds.; Academic Press: New York, 1978; p 412.
(27) Collins, J. M.; Gillespie, R. J. *Inorg. Chem.* **1984**, *23*, 1975.
(28) Sheldrick, G. M. *Crystallographic Computing 3*; Oxford University Press: Oxford, U.K., 1985; p 175.

Table I. Crystallographic Parameters for **1**, **4**, and **7**

	1	**4**	**7**
formula	$C_{18}H_{54}Si_8Te_2Zn$	$C_{28}H_{64}N_2Si_8Te_2Zn$	$C_{24}H_{70}P_2Si_8Te_2Cd$
mol wt	815.89	974.1	1013.05
space group	$P\bar{1}$	$P\bar{1}$	$P2_12_12_1$
a/Å	14.804 (5)	11.9191 (22)	13.1498 (21)
b/Å	16.458 (5)	12.1397 (16)	25.5525 (34)
c/Å	18.237 (5)	17.319 (3)	28.5349 (36)
α/deg	63.97 (2)	105.328 (13)	90.0
β/deg	84.61 (2)	99.711 (16)	90.0
γ/deg	79.47 (2)	96.278 (12)	90.0
vol/Å^3	3925.0 (25)	2350.7 (16)	9588.0 (23)
Z	2	2	8
d_{calcd}/g cm^{-3}	1.38	1.38	1.40
cryst size/mm	0.3 × 0.2 × 0.2	0.26 × 0.32 × 0.50	0.6 × 0.25 × 0.35
radiation type (λ/Å)	Mo Kα (0.710 73)	Mo Kα (0.710 73)	Mo Kα (0.710 73)
scan mode	θ–2θ	θ–2θ	θ–2θ
2θ range/deg	3–45	2–45	3–45
collection range	$+h,\pm k,\pm l$	$+h,\pm k,\pm l$	$+h,+k,+l$
abs coeff, μ	23.5	19.7	19.3
no. of unique reflns	10 709	6130	6914
no. of reflns with $F^2 > 3\sigma(F^2)$	7404	5350	5795
final R, R_w	0.0308, 0.0319	0.0278, 0.0362	0.027, 0.029
T/°C	−105	−71	−117

thermal parameters were refined by the block-diagonalized-matrix least-squares method. The minimized function was $\sum w(|F_o| - |F_c|)^2$, where w is the weight of a given observation. The p factor, used to reduce the weight of intense reflections, was set to 0.03 throughout the refinement. In the final cycle of the refinement, all parameter shift/error values were less than 0.01σ. The analytical forms of the scattering factor tables for the neutral atoms were used, and all scattering factors were corrected for both real and imaginary components of anomalous dispersion. The largest peaks in the final difference Fourier maps for **1**, **4**, and **7** were 1.40, 1.50, and 0.74 e/Å^3, respectively, and the lowest excursions were −0.12, −0.11, and −0.12 e/Å^3, respectively. A summary of data collection and refinement parameters is given in Table I. Positional and thermal parameters of the non-hydrogen atoms for each compound are given as supplementary material. The structure of **4** was determined by Dr. F. J. Hollander at the UC Berkeley College of Chemistry X-ray facility, CHEXRAY.

{Zn[TeSi(SiMe$_3$)$_3$]$_2$}$_2$ (1). Transparent, green-yellow, blocky crystals were obtained by slow crystallization from hexane at −40 °C. A suitable fragment was cleaved from one large block and was mounted on a glass fiber using Paratone N hydrocarbon oil. The crystal was transferred to an Enraf-Nonius CAD-4 diffractometer, centered in the beam, and cooled to −105 °C. The unit cell was determined to be primitive triclinic with space group $P\bar{1}$. The 10 709 unique raw intensities were converted to structure factor amplitudes and their esd's by correction for scan speed, background, and Lorentz and polarization effects. Hydrogen atoms were assigned idealized locations and were included in structure factor calculations, but were not refined. The final residuals for 523 variables refined against the 7404 data for which $F^2 > 3\sigma(F^2)$ were R = 0.0308, R_w = 0.0319, and GOF = 1.146. The R value for all 10 709 data was 0.0613.

Zn[TeSi(SiMe$_3$)$_3$]$_2$(pyr)$_2$ (4). Transparent, yellow, cubic crystals were obtained by slow crystallization from dichloromethane at −40 °C. A fragment cleaved from one of these crystals was mounted as described above. The crystal was centered in the beam and cooled to −71 °C. The unit cell was determined to be primitive triclinic with space group $P\bar{1}$. The 6130 unique raw intensities were manipulated as described above. In a difference Fourier map calculated following the refinement of all non-hydrogen atoms with anisotropic thermal parameters, peaks were found corresponding to the positions of all of the hydrogen atoms. Hydrogen atoms were assigned idealized locations and values of B_{iso} approximately 1.15 times the B_{equ} of the atoms to which they were bonded. They were included in structure factor calculations, but were not refined. The final residuals for 371 variables refined against the 5350 data for which $F^2 > 3\sigma(F^2)$ were R = 0.0278, R_w = 0.0362, and GOF = 1.76. The R value for all 6130 data was 0.0340.

Cd[TeSi(SiMe$_3$)$_3$]$_2$(dmpe) (7). Transparent, yellow, blocky crystals were obtained by slow crystallization from dichloromethane at −40 °C. A single crystal was halved and was mounted as described above. The crystal was centered in the X-ray beam and cooled to −117 °C. The unit cell was determined to be primitive monoclinic with space group $P2_12_12_1$. Hydrogen atoms were assigned idealized locations and were included in structure factor calculations, but were not refined. The final residuals for 667 variables refined against the 5795 data for which $F^2 > 3\sigma(F^2)$ were R = 0.027, R_w = 0.029, and GOF = 1.09. The R value for all 6914 data was 0.039.

Results and Discussion

Preparation of Homoleptic Tellurolates. The tellurolysis reaction between HTeSi(SiMe$_3$)$_3$ and group 12 amides in nonpolar hydrocarbons, such as pentane or hexane, provides a straightforward, high-yield route to the homoleptic tellurolates of zinc, cadmium, and mercury (eq 1). Alternatively, tellurolysis of Zn–C bonds

$$2HTeSi(SiMe_3)_3 + M[N(SiMe_3)_2]_2 \rightarrow \underset{\mathbf{1-3}}{M[TeSi(SiMe_3)_3]_2} + 2HN(SiMe_3)_2 \quad (1)$$

M = Zn (**1**), Cd (**2**), Hg (**3**)

is equally facile (eq 2). The choice of a nondonor solvent provides

$$2HTeSi(SiMe_3)_3 + ZnEt_2 \rightarrow Zn[TeSi(SiMe_3)_3]_2 + 2C_2H_6 \quad (2)$$

for a simple workup procedure, consisting of removal of all volatile components followed by crystallization from concentrated hexane or hexamethyldisiloxane at −40 °C. Although isolated yields range from 67 to 90%, these are still lower than expected on the basis of reactions monitored by ^{1}H NMR spectroscopy, where conversion to products appeared quantitative. The high solubility of the compounds is no doubt to blame for this diminution in isolated yield. It is worth noting that attempts to prepare these compounds by conventional metathesis reactions were thwarted by a number of practical difficulties. In the preparation of **1**, for example, reaction between 2 equiv of (THF)$_2$LiTeSi(SiMe$_3$)$_3$ and $ZnCl_2$ in hexane, toluene, or THF invariably led to isolation of complexes containing coordinated THF. Small-scale reactions of (THF)$_2$LiTeSi(SiMe$_3$)$_3$ with $CdBr_2$ in diethyl ether did afford samples of the base-free compound; however, on larger scales, **2** was frequently contaminated with coordinated solvent. Metathesis between (THF)$_2$LiTeSi(SiMe$_3$)$_3$ and $HgCl_2$ in diethyl ether was more successful, although yields were lower than those afforded by tellurolysis (ca. 60–67%). Clearly, these trends follow the decreasing Lewis acidity as we proceed down group 12 from zinc to mercury.

The homoleptic compounds are yellow or yellow-green, highly crystalline solids that are stable indefinitely when stored under N_2 at ambient temperature and normal room lighting. The surface of crystalline **3** becomes dark green-black under these conditions; however, the material remains spectroscopically and analytically pure. As solids, the compounds show varying degrees of air sensitivity, with the observed trend mirroring the Lewis acidity of the metal center. Thus, whereas **1** oxidizes almost instantly to the ditelluride $Te_2[Si(SiMe_3)_3]_2$ on exposure to air (as determined by ^{1}H NMR spectroscopy), the mercury derivative, **3**, remains spectroscopically pure even after 45 min. They are thermally stable and may be sublimed without decomposition at

Table II. $^{125}Te\{^1H\}$ NMR Data for New Compounds[a]

cmpd	solvent	T/°C	concn/(mol/L)	δ_{Te}/ppm	$\Delta\nu_{1/2}$/Hz	comments
1	C_7D_8	−60	0.22	−783 (brdg)	260	
				−1215 (term.)	260	
2	C_7D_8	−65	0.36	−933 (brdg)	130	$\lvert J_{TeCd}\rvert$ = 1059 Hz $\lvert J_{TeSi}\rvert$ = 275 Hz
				−1338 (term.)	90	$\lvert J_{Te^{111}Cd}\rvert$ = 1821 Hz $\lvert J_{Te^{113}Cd}\rvert$ = 1897 Hz
3	C_7D_8	−90	0.36	−850	30	J_{TeH_g} not obsd $\lvert J_{TeSi}\rvert$ = 248 Hz
4	$CDCl_3$	25	0.21	−1469	101	
7	CD_2Cl_2	−40	0.21	−1565	19	$\lvert J_{TeCd}\rvert$ = 744 Hz $\lvert {}^2J_{TeP}\rvert$ = 137 Hz

[a] Relative to external neat Me_2Te at 0 ppm.

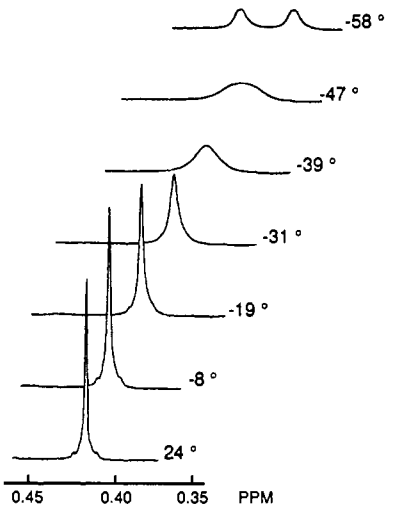

Figure 1. Variable-temperature ^1H NMR spectra of $\{Cd[TeSi(SiMe_3)_3]_2\}_2$ (**2**).

elevated temperatures under reduced pressure (10^{-3} Torr, ca. 200 °C). Experiments using these compounds as precursors to metal tellurides via chemical vapor deposition will be described in a future publication. All three homoleptic compounds are exceedingly soluble in hydrocarbon, ethereal, or chlorinated solvents and are stable indefinitely in the absence of water and O_2; exposure to dry oxygen gives the ditelluride in quantitative yield as judged by ^1H NMR spectroscopy.

Characterization of **1**–**3** is based on elemental analysis, MS, IR, and NMR spectroscopy, and X-ray crystallography. Signals due to the monomers $M[Si(SiMe_3)_3]_2$ are observed for all three compounds under standard EI or FAB MS conditions. No evidence for higher molecular weight species was found. In each case, ions at m/z 750 and 677, due to the ditelluride $Te_2[Si(SiMe_3)_3]_2$ followed by loss of an $-SiMe_3$ group, were observed. In addition, peaks at m/z 623, 551, and 478 correspond to the disilyltelluride $Te[(SiMe_3)_3]_2$ followed by loss of one and two $-SiMe_3$ groups, respectively. IR spectra of **1**–**3** are remarkably similar, comprising mainly peaks due to the tellurolate ligand.

Multinuclear NMR spectroscopy provides valuable information as to the structures present in solution. The proton NMR spectra of **1**–**3** at 20 °C show a single peak at 0.3–0.4 ppm in toluene-d_8. On cooling, however, the signals for **1** and **2** broaden before splitting into two singlets of equal intensity. Decoalescence occurs at −50 and −34 °C for **1** and **2**, respectively; Figure 1 displays the results for the cadmium derivative. No evidence for decoalescence was detected in the case of **3**, even down to −90 °C. These data are consistent with a dimeric, tellurolate-bridged structure, at least for **1** and **2**, in which bridge–terminal exchange is slowed (relative to the NMR time scale) at low temperature.

As concentrated solutions of these compounds were readily prepared (typically 100–200 mg in 0.5 mL of benzene), observation of informative $^{125}Te\{^1H\}$ NMR spectra (^{125}Te; $I = {}^1/_2$, 6.99%) became relatively straightforward; these data (Table II) lend further support to the arguments above. The room-temperature

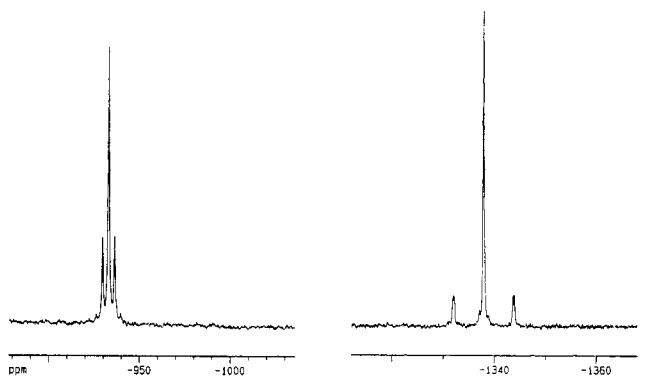

Figure 2. $^{125}Te\{^1H\}$ NMR spectrum of $\{Cd[TeSi(SiMe_3)_3]_2\}_2$ (**2**) at −65 °C.

^{125}Te NMR spectra of **1** and **2** in toluene-d_8 are featureless; however, when the samples are cooled to 0 °C, two distinct resonances appear that sharpen considerably on further cooling to ca. −60 °C. We assign these two peaks to tellurium atoms in bridging and terminal sitel ligands. For the zinc derivative **1**, the high-field resonance at −1215 ppm is due to the terminal sitel ligand, which is shielded relative to the bridging ligand, whose resonance appears at −783 ppm. These assignments become even more straightforward on analysis of spectra for the homoleptic cadmium compound **2** (Figure 2). Now the tellurium nuclei couple to both ^{113}Cd ($I = {}^1/_2$, 12.26%) and ^{111}Cd ($I = {}^1/_2$, 12.75%), giving rise to two sets of satellites that provide valuable structural information. Consideration of relative isotopomeric distributions predict a three-line pattern for a terminal tellurium signal and a five-line pattern for a bridging tellurolate. The former is observed at −1338 ppm ($\Delta\nu_{1/2}$ = 40 Hz) and the latter at −933 ppm ($\Delta\nu_{1/2}$ = 90 Hz). The upfield shift is now unambiguously assigned to the terminal tellurolate on the basis of the intensity and multiplicity of the satellites. The higher s character of the Cd–Te(terminal) bond gives rise to a much higher coupling constant than that for the Cd–Te(bridge) interaction. Interestingly, the cadmium satellites of the terminal tellurolate show distinct resonances for ^{113}Cd and ^{111}Cd. Because coupling constants are directly proportional to nuclear frequencies (^{113}Cd resonates at a higher nuclear frequency than ^{111}Cd; 110.948 MHz vs 106.049 MHz in our experiments), we can assign the larger coupling constant to ^{125}Te–^{113}Cd, such that $\lvert J_{Te^{111}Cd}\rvert$ = 1821 Hz and $\lvert J_{Te^{113}Cd}\rvert$ = 1897 Hz. Because its natural line width was larger, such distinctions were not apparent for the bridging sitel ligand, whose average $\lvert J_{Te^{111/113}Cd}\rvert$ = 1059 Hz.

The $^{113}Cd\{^1H\}$ NMR spectrum serves to further confirm these assignments. A concentrated solution of **2** in toluene-d_8 at −71 °C shows a relatively sharp singlet at δ 117 ppm ($\Delta\nu_{1/2}$ = 69 Hz) flanked by two sets of ^{125}Te satellites. $\lvert J_{^{113}Cd^{125}Te}\rvert$ for the bridging sitel is 1088 Hz, while that for the terminal sitel is 1904 Hz. At ambient temperature in benzene-d_6, a broad ^{113}Cd resonance was detected at δ 97 ppm ($\Delta\nu_{1/2}$ = 240 Hz) with no observable coupling to tellurium.

As expected on the basis of proton data, $^{125}Te\{^1H\}$ spectra of **3** show only a single line at −850 ppm ($\Delta\nu_{1/2}$ = 20 Hz) from +80

to −80 °C. No mercury satellites were observed in any of these spectra. Coupling to ^{29}Si was apparent, however, with $|J_{TeSi}|$ = 248 Hz (^{29}Si; $I = {}^1/_2$, 4.71%); this is similar in magnitude to the values determined for **2** (275 Hz), $(SiMe_3)_3SiTeTeSi(SiMe_3)_3$ (289 Hz), and $Me_3SiTeSi(SiMe_3)_3$ (316 Hz).[21] The lack of Te–Hg coupling was also mirrored in the ambient-temperature $^{199}Hg\{^1H\}$ NMR spectrum of **3** (^{199}Hg; $I = {}^1/_2$, 16.84%), where only a singlet with no ^{125}Te satellites was observed at −2328 ppm ($\Delta\nu_{1/2}$ = 23 Hz). Analysis of NMR data for **3**, therefore, cannot distinguish between a monomeric structure and a dimer in which bridge–terminal exchange is rapid on the NMR time scale. As mentioned earlier, there are few reports of well-characterized mercury tellurolates. These include the aryl derivatives $Hg(TeC_6H_4R)_2$ (R = H,[12] OEt,[29] Me[30]) and the fluoroaryl compound $Hg(TeC_6F_5)_2$.[31] Dean and co-workers have characterized a number of adamantane-like cage compounds containing the cations $[(\mu\text{-}TeR)_6(HgL)_4]^{2+}$ (L = phosphine, arsine),[32] and the structure of $[Ph_4P][Hg(TePh_3)]$ was described some time ago.[33,34] Some alkyl derivatives are known,[12,35] and very recently, a more thorough investigation of the chemistry of mercury aryltellurolates was reported.[13]

Further evidence that **1**–**3** are aggregated to varying degrees in solution is supported by vapor pressure molecular weight measurements. Calculated molecular weights for monomeric **1**–**3** are 816, 863, and 951, respectively. However, the average experimentally determined values for **1**–**3** as 10^{-2} M solutions in benzene were 913, 1113, and 901, corresponding to degrees of association of 1.12, 1.29, and 0.95 for **1**–**3**, respectively. These results mirror the trend observed by NMR spectroscopy, suggesting that the tendency for dimerization increases in the order Cd > Zn > Hg. On the basis of considerations of Lewis acidity of the metal ion alone, however, we would expect to see the zinc complex forming the strongest dimer. Given the available evidence, we tentatively ascribe this apparent anomaly to greater interligand repulsion in the zinc derivative due to its smaller radius compared to cadmium. Alternatively, cadmium, being a softer Lewis acid, binds more readily to the soft tellurium donor in the bridging sitel ligand. Confirmation of a dimeric structure for **1** is provided by X-ray crystallography (see below).

Donor Complexes. The existence of a monomer–dimer equilibrium suggested that addition of good Lewis bases might perturb this process and lead to the formation of monomeric donor adducts. Two equivalents of monodentate bases such as pyridine and PMe_3 rapidly add to the zinc center in **1** to form four-coordinate species. Compared to their homoleptic precursor, these donor complexes are markedly less air-sensitive and are, in general, less soluble in hydrocarbons. The pyridine adduct **4**, for example, precipitates from hexane as it is formed and is best purified from CH_2Cl_2, from which it crystallizes as clear yellow cubes. Ambient-temperature $^{125}Te\{^1H\}$ NMR data show a sharp singlet at −1469 ppm ($\Delta\nu_{1/2}$ = 51 Hz). A tetrahedral geometry has been confirmed by X-ray crystallography (see below). In the case of the cadmium complex **2**, 2 equiv of pyridine, 4-*tert*-butylpyridine, and PMe_3 form related adducts cleanly in high yield, as judged by ^1H and $^{31}P\{^1H\}$ NMR spectroscopy.

Bidentate ligands such as dmpe and bpy readily coordinate to the metal centers in **1** and **2** to form stable donor complexes. For zinc, the bpy complex **5** was isolated in 71% yield as orange-red crystals. Bright yellow crystalline bpy (**6**) and dmpe (**7**) adducts of the cadmium tellurolate were also isolated in high yields.

For the cadmium complexes, there is evidence for dynamic behavior in solution from NMR spectroscopy. In the bpy adduct **6**, for example, addition of excess ligand (1–4 mol equiv) results in the appearance of four broad bpy resonances in the ^1H NMR spectrum that are shifted from those in the pure compound; these signals sharpen on raising the temperature to 60 °C. The positions of these peaks vary with the amount of added bpy, such that a weighted average signal between free and complexed ligand is observed. Clearly, ligand exchange is rapid on the NMR time scale at room temperature. Conclusions based on related experiments with **5** are complicated by its relatively rapid decomposition soon after dissolution; however, when excess bpy was added, distinct resonances for both free and complexed ligands were observed, suggesting that the exchange in this case is much slower. Unfortunately, the relative insolubility of compounds **5** and **6** precluded observation of ^{125}Te NMR spectra.

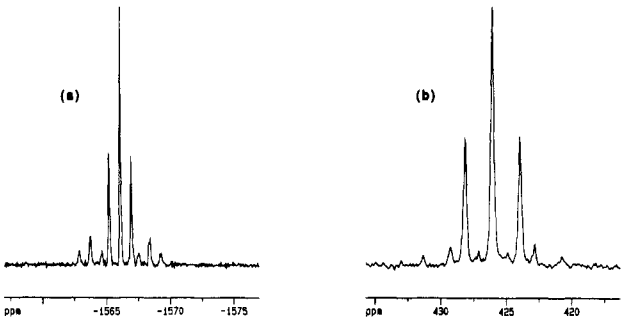

Figure 3. (a) $^{125}Te\{^1H\}$ and (b) $^{113}Cd\{^1H\}$ NMR spectra of $Cd[TeSi(SiMe_3)_3]_2(dmpe)$ (**7**) at −40 and −70 °C, respectively.

The cadmium dmpe adduct (**7**) also appears to be labile in solution. No $^{125}Te\{^1H\}$ NMR signal could be detected at room temperature in dichloromethane-d_2; however, at −40 °C, a sharp triplet was observed at δ −1566 ppm ($\Delta\nu_{1/2}$ = 19 Hz) (see Figure 3a). In addition to coupling from the two equivalent ^{31}P nuclei ($|^2J_{TeP}|$ = 137 Hz), we also begin to see distinct ^{113}Cd and ^{111}Cd satellites, with $|J_{Te^{113}Cd}|$ = 748 Hz and $|J_{Te^{111}Cd}|$ = 714 Hz. These coupling constants are noticeably smaller than those observed for the homoleptic derivative **2**, where $|J_{^{125}Te^{113}Cd}|$ values of 1059 and 1897 Hz were found for the bridging and terminal sitel ligands, respectively.

The room-temperature $^{31}P\{^1H\}$ NMR spectrum of **7** shows only a singlet at δ −47.2 ppm with no coupling to other nuclei. The similarity of this value to that for free dmpe (δ −49.7 ppm[22,36]) implies that the phosphine is only weakly coordinated. On cooling, the resonance broadens considerably and shifts to δ −40 ppm ($\Delta\nu_{1/2}$ = 8 Hz) with coupling to cadmium and tellurium resolvable by −70 °C. At −90 °C, these signals sharpen to the point where phosphorus couplings to ^{113}Cd, ^{111}Cd, ^{125}Te, and ^{123}Te (^{123}Te; $I = {}^1/_2$, 0.87%) are all resolved. Just as the ratios of the P–^{113}Cd and P–^{111}Cd coupling constants (251 and 240 Hz, respectively) scale as the ratios of the different cadmium NMR frequencies, so in turn do the ratios of the P–^{125}Te and P–^{123}Te coupling constants (140 and 114 Hz, respectively).

At room temperature, the $^{113}Cd\{^1H\}$ NMR spectrum of **7** consists of a singlet at δ 371 ppm ($\Delta\nu_{1/2}$ = 30 Hz) with what appear to be tellurium satellites ($|J_{^{113}Cd^{125}Te}|$ = 799 Hz) (Figure 3b). Again the spectrum is sharper at −70 °C, where a triplet at δ 421 ppm ($|J_{^{113}CdP}|$ = 233 Hz) is flanked by ^{125}Te satellites with $|J_{^{113}Cd^{125}Te}|$ = 711 Hz. These values correlate well with the equivalent couplings from $^{125}Te\{^1H\}$ and $^{31}P\{^1H\}$ NMR spectra. Further proof of the structure of the complex is provided by X-ray crystallography, as described below.

In accord with the low Lewis acidity of the mercury derivative **3**, preparative-scale reactions between this compound and pyr, bpy, or PMe_3 led only to isolation of the uncomplexed mercury tellurolate and free base. In NMR tube reactions in benzene-d_6, no changes were observed in the ^1H NMR spectra of the starting materials.

X-ray Crystallography. The molecular structure of **1** is shown as an ORTEP view in Figure 4, with pertinent bond lengths and

(29) Dance, N. S.; Jones, C. H. W. *J. Organomet. Chem.* **1978**, *152*, 175.
(30) Steigerwald, M. L.; Sprinkle, C. R. *J. Am. Chem. Soc.* **1987**, *109*, 7200.
(31) Kasemann, R.; Naumann, D. *J. Fluorine Chem.* **1990**, *48*, 207.
(32) Dean, P. A. W.; Manivannan, V. *Inorg. Chem.* **1990**, *29*, 2997. Dean, P. A. W.; Manivannan, V. *Can. J. Chem.* **1990**, *68*, 214. Dean, P. A. W.; Manivannan, V.; Vittal, J. J. *Inorg. Chem.* **1989**, *28*, 2360.
(33) Liesk, J.; Klar, G. *Z. Anorg. Allg. Chem.* **1977**, *435*, 103.
(34) Liesk, J.; Schulz, P.; Klar, G. *Z. Anorg. Allg. Chem.* **1977**, *435*, 98.
(35) Harris, D. C.; Nissan, R. A.; Higa, K. T. *Inorg. Chem.* **1987**, *26*, 765.
(36) Dixon, K. R. In *Multinuclear NMR*; Mason, J., Ed.; Plenum Press: New York, 1989; p 369.

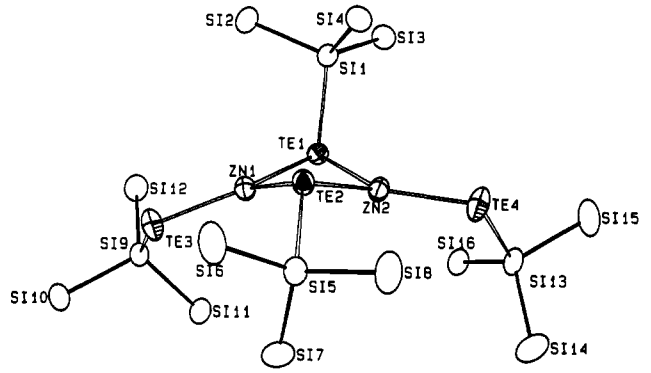

Figure 4. ORTEP view of $\{Zn[TeSi(SiMe_3)_3]_2\}_2$ (**1**). Methyl groups are omitted for clarity, and the thermal ellipsoids are drawn at the 50% probability level.

Table III. Selected Bond Distances (Å) and Angles (deg) for **1**

Zn1–Te1	2.634 (1)	Zn1–Te2	2.628 (1)
Zn1–Te3	2.490 (1)	Zn2–Te1	2.649 (1)
Zn2–Te2	2.650 (1)	Zn2–Te4	2.500 (1)
Te1–Si1	2.570 (2)	Te2–Si5	2.534 (2)
Te3–Si9	2.516 (2)	Te4–Si13	2.516 (2)
Si1–Si2	2.353 (2)	Si1–Si3	2.356 (2)
Si1–Si4	2.360 (2)	Si2–C1	1.869 (8)
Si2–C2	1.857 (8)	Si2–C3	1.861 (7)
Zn1–Te1–Zn2	79.25 (2)	Zn1–Te1–Si1	105.48 (4)
Zn2–Te1–Si1	97.43 (4)	Zn1–Te2–Zn2	79.33 (3)
Zn1–Te2–Si5	115.63 (5)	Zn2–Te2–Si5	115.79 (5)
Zn1–Te3–Si9	110.33 (5)	Zn2–Te4–Si13	113.00 (5)
Te1–Zn1–Te2	96.06 (3)	Te1–Zn1–Te3	140.89 (3)
Te2–Zn1–Te3	122.98 (3)	Te1–Zn2–Te2	95.18 (3)
Te1–Zn2–Te4	137.70 (3)	Te2–Zn2–Te4	125.12 (3)
Te1–Si1–Si2	105.67 (8)	Te1–Si1–Si3	100.04 (8)
Te1–Si1–Si4	120.52 (8)	Si2–Si1–Si3	111.63 (9)
Si2–Si1–Si4	107.98 (9)	Si3–Si1–Si4	110.76 (9)

angles given in Table III. The X-ray structures of **1** and **4** (see below) are the first such reports for zinc tellurolates. Compound **1** crystallizes in space group $P\bar{1}$, and thus only inversion symmetry between the two asymmetric units is observed. Although higher symmetry appears to be present, minor variations in the bulky $-Si(SiMe_3)_3$ groups destroy these elements. The Zn_2Te_2 core of the dimer is butterflied; both Zn–Te–Zn angles are acute [79.25 (2), 79.33 (3)°], while the two Te–Zn–Te angles are only slightly obtuse [95.18 (3), 96.06 (3)°]. The bridging tellurium atoms are clearly pyramidal, presumably due to the repulsion between the lone pairs and bonding electrons. A bent geometry, consistent with sp^3 hybridization, is observed for the tellurium atoms in the terminal sitel ligands, with Zn–Te–Si angles of 110.55 (5) and 113.00 (5)°. The geometry at each zinc is trigonal planar: the Te–Zn–Te angles about Zn1 total 359.9°, while those about Zn2 sum to 358.0°. Inspection of bond lengths in the Zn_2Te_2 core, which range from 2.628 (1) to 2.650 (1) Å, indicates that the bridging sitel ligands are quite symmetrically disposed. These values are significantly longer than the average Zn–Te(terminal) bond lengths (2.50 Å), perhaps as a result of greater interligand repulsion between the bulky sitel groups. Average Te–Si distances in both bridging and terminal tellurolates are similar at 2.552 and 2.516 Å, respectively. Complexes related to **1** include the homoleptic selenolate $[Cd(SeAr)_2]_2$ (Ar = 2,4,6-^{t}Bu$_3$Ph) and the corresponding thiolate $[Cd(SAr)_2]_2$.[16,37] It is interesting to note that the Cd_2Se_2 and Cd_2S_2 cores in these compounds are planar.

Figure 5 shows an ORTEP drawing of the bis(pyridine) adduct **4**, which also crystallizes in the space group $P\bar{1}$. A nearly 2-fold symmetry in the molecule exists, but again, this higher symmetry is broken by the orientation of the $-SiMe_3$ groups and only inversion symmetry is present. The geometry about the four-coordinate Zn center may be viewed as a distorted tetrahedron, with

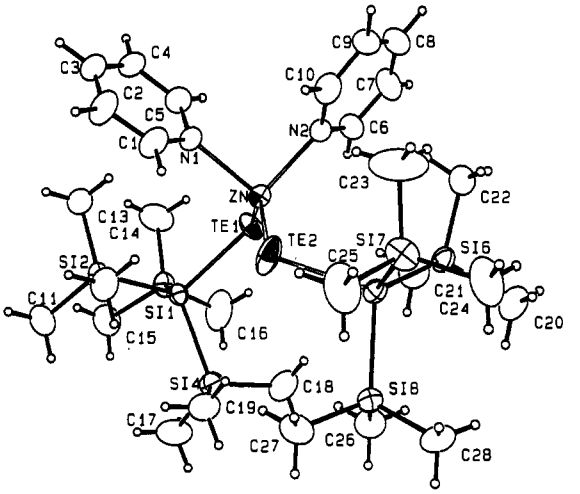

Figure 5. ORTEP view of $Zn[TeSi(SiMe_3)_3]_2(pyr)_2$ (**4**). Thermal ellipsoids are drawn at the 50% probability level.

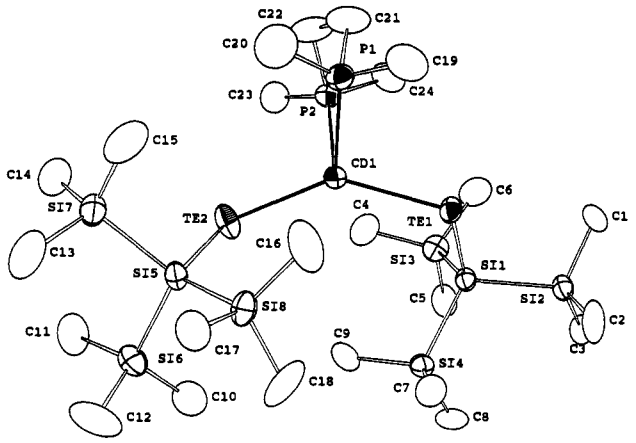

Figure 6. ORTEP view of $Cd[TeSi(SiMe_3)_3]_2(dmpe)$ (**7**). Hydrogens are omitted for clarity, and the thermal ellipsoids are drawn at the 50% probability level.

Table IV. Selected Bond Distances (Å) and Angles (deg) for **4**

Zn–Te1	2.579 (1)	Zn–Te2	2.569 (1)
Zn–N1	2.142 (3)	Zn–N2	2.124 (3)
Te1–Si1	2.506 (1)	Te2–Si5	2.506 (1)
Si1–Si2	2.338 (1)	Si1–Si3	2.345 (1)
Si1–Si4	2.349 (1)	Si8–C26	1.857 (5)
Si8–C27	1.869 (5)	Si8–C28	1.872 (4)
N1–C1	1.326 (5)	N1–C5	1.338 (5)
N2–C6	1.323 (5)	N2–C10	1.335 (5)
Te1–Zn–Te2	131.92 (2)	Te1–Zn–N1	107.87 (8)
Te1–Zn–N2	100.79 (8)	Te2–Zn–N1	102.39 (8)
Te2–Zn–N2	113.70 (8)	N1–Zn–N2	93.73 (12)
Zn–Te1–Si1	109.21 (3)	Zn–Te2–Si5	112.90 (3)
Te1–Si1–Si2	112.47 (5)	Te1–Si1–Si3	100.85 (5)
Te1–Si1–Si4	110.14 (5)	Si2–Si1–Si3	110.25 (6)
Si2–Si1–Si4	112.87 (6)	Si3–Si1–Si4	109.61 (6)

angles ranging from a minimum of 93.7 (1)° for the N–Zn–N interaction to a maximum of 131.92 (2)° for the Te–Zn–Te interaction (Table IV). Steric repulsion by the large sitel ligands is the simplest explanation for these deviations. The Zn–N bond lengths [2.142 (3), 2.124 (3) Å] are ca. 0.1 Å longer than those found in related zinc pyridine compounds, such as $Zn[S_2P(O-{}^iPr)_2]_2(pyr)$ and $Zn(pyr)_2(NO_2)_2$ (Zn–N = 2.028 (4) and 2.062 (3) Å, respectively),[38,39] or than the bond length predicted on the

(37) Bochmann, M.; Webb, K. J.; Hursthouse, M. B.; Mazid, M. *J. Chem. Soc., Dalton Trans.* **1991**, 2317.

(38) Hitchman, M. A.; Thomas, R.; Skelton, B. W.; White, A. H. *J. Chem. Soc., Dalton Trans.* **1983**, 2273.

(39) Harrison, P. G.; Begley, M. J.; Kikabhai, T. *J. Chem. Soc., Dalton Trans.* **1986**, 929.

Table V. Selected Bond Distances (Å) and Angles (deg) for 7

Te1-Cd1	2.744 (1)	Te1-Si1	2.519 (2)
Te2-Cd1	2.722 (1)	Te2-Si5	2.512 (3)
Cd1-P1	2.691 (2)	Cd1-P2	2.724 (3)
P1-C19	1.778 (11)	P1-C20	1.793 (12)
P1-C21	1.827 (11)	P2-C22	1.828 (10)
P2-C23	1.821 (11)	P2-C24	1.830 (11)
P1-Cd1-P2	78.50 (8)	P1-Cd1-Te1	97.01 (6)
P2-Cd1-Te2	108.98 (6)	P1-Cd1-Te2	115.41 (6)
P2-Cd1-Te2	96.37 (6)	Te1-Cd1-Te2	142.35 (3)
Cd1-Te1-Si1	107.55 (6)	Cd1-Te2-Si5	113.68 (6)
Cd1-P1-C19	118.6 (4)	Cd1-P1-C20	123.8 (5)
Cd1-P1-C21	104.2 (4)	Te1-Si1-Si2	102.27 (10)
Te1-Si1-Si3	114.12 (12)	Te1-Si1-Si4	109.95 (12)

basis of ionic radii (2.01 Å).[40] The Zn-Te bond lengths [2.579 (1) and 2.569 (1) Å] lie between the values determined for terminal and bridging Zn-Te interactions observed in **1**.

In order to remove any ambiguity regarding the structure of the labile cadmium-dmpe adduct **7** (see above), its crystal structure has also been determined. The compound crystallizes in the space group $P2_12_12_1$ with two independent molecules per asymmetric unit. Figure 6 shows an ORTEP view of molecule 1; metrical parameters for the two are identical within experimental error (see Table V). The smallest angle about the pseudotetrahedral cadmium is that due to the bidentate dmpe ligand, which makes a P-Cd1-P angle of 78.50 (8)°. The Te-Cd1-Te angle [142.35 (3)°] is somewhat larger than the corresponding angle in **1**. The Cd1-P bond distances [2.691 (2), 2.724 (3) Å] compare to those in the polymeric selenolate complex $\{Cd_2(\mu\text{-SePh})_2(SePh)_2](depe)\}_\infty$,[15] where the Cd-P bond length is 2.582 (7) Å. A slight difference in the Cd1-Te bond lengths [2.744 (1) and 2.722 (1) Å] was observed. Only one other cadmium tellurolate has been structurally characterized: the mesityl derivative $[Cd(TeMe_3C_6H_2)_2]_\infty$, which exists as a coordination polymer with bridging mesityl tellurolates. Both the Cd and Te atoms are three-coordinate in this compound, and hence the Cd-Te bond lengths [average 2.837 (9) Å] are significantly longer than those found in **7**.

Conclusions. The sterically demanding sitel anion has been shown to act as a versatile ligand for the formation of novel tellurolate derivatives of zinc, cadmium, and mercury. Compared to related aryltellurolates, the sitel derivatives exhibit a number of appealing characteristics, including their ease of preparation and handling, high crystallinity, and exceptional solubility in hydrocarbon solvents. In addition, their low molecularity and relatively high volatility render them of interest as single-source precursors to II/VI thin-film semiconductors. The results of these studies, and our efforts to extend sitel chemistry to a wider variety of metal compounds, will be described in subsequent publications.

Acknowledgment. We thank Dr. Frederick J. Hollander and Virginia A. Carlson for their assistance with X-ray crystallography and Dr. Graham E. Ball for his invaluable and enthusiastic help with NMR experiments. Financial support from the National Science Foundation (Grant CHE-90-19675), the Department of Education, and UC Berkeley is gratefully acknowledged.

Supplementary Material Available: Details of the structure determinations of **1**, **4**, and **7**, including tables of temperature factor expressions, positional parameters, and intramolecular distances and angles (38 pages); listings of observed and calculated structure factors (136 pages). Ordering information is given on any current masthead page.

(40) Shannon, R. D.; Prewitt, C. T. *Acta Crystallogr.* **1969**, *B25*, 925. Shannon, R. D. *Acta Crystallogr.* **1976**, *A32*, 751.

Contribution from the Department of Chemistry, State University of New York at Stony Brook, Stony Brook, New York 11794-3400

Kinetic, Isotopic, and ^{15}N NMR Study of *N*-Hydroxybenzenesulfonamide Decomposition: An HNO Source Reaction

Francis T. Bonner* and Younghee Ko

Received December 26, 1991

Decomposition of *N*-hydroxybenzenesulfonamide ($C_6H_5SO_2NHOH$) in alkaline solution to yield N_2O and sulfinate ($C_6H_5SO_2^-$) is first order in $C_6H_5SO_2NHO^-$, with rate constant = 2.44 (±0.23) × 10^{-4} s^{-1} at 25 °C, $\Delta H^\ddagger$ = 94.1 kJ mol^{-1}, and $\Delta S^\ddagger$ = 6.64 J K^{-1} mol^{-1}. The reaction occurs via reversible release of HNO (and/or its conjugate NO^-), followed by rapid dimerization of the intermediate to form N_2O. It is shown by ^{15}N tracer methods that this species and the NO^- intermediate formed in trioxodinitrate decomposition are capable of codimerization, showing them to be in the same (singlet) electronic state. Protonation of $C_6H_5SO_2NHO^-$ brings about a ^{15}N NMR shift of −28.6 ppm. The free acid and its basic anion exhibit identical, large NOEF values (−4.16), showing that the dissociable hydrogen in $C_6H_5SO_2NHOH$ is bound to oxygen rather than to nitrogen, despite contrary literature reports.

Preparation of *N*-hydroxybenzenesulfonamide ($C_6H_5SO_2NHOH$, "Piloty's acid") was first reported in 1896.[1] In alkaline aqueous solution this compound undergoes self-decomposition to yield nitrous oxide and benzenesulfinate (eq 1).

$$C_6H_5SO_2NHOH(aq) + OH^-(aq) \rightarrow \tfrac{1}{2}N_2O(g) + C_6H_5SO_2^-(aq) + 1\tfrac{1}{2}H_2O \quad (1)$$

It was first postulated by Angeli[2] that this reaction occurs via elimination of HNO ("nitroxyl") from the conjugate anion (eqs 2 and 3), analogous to the self-decomposition of trioxodinitrate

$$C_6H_5SO_2NHO^- \rightarrow HNO + C_6H_5SO_2^- \quad (2)$$

$$HNO + HNO \rightarrow N_2O + H_2O \quad (3)$$

($Na_2N_2O_3$, "Angeli's salt").[3] This is one of several examples in the literature of organic chemistry for which HNO elimination is strongly indicated. Others include the nitrosative degradation of tertiary amines,[4] conversion of aliphatic secondary nitro compounds to aldehydes or ketones via acid-catalyzed solvolysis,[5] a retro Diels-Alder reaction;[6] and HNO elimination from certain *N*-nitroso organophosphorus compounds.[7] Alkaline *N*-hydroxybenzenesulfonamide is a key reagent in the well-known Angeli-Rimini test for aldehydes,[8] but it has been shown by Smith

(1) Piloty, O. *Ber. Dtsch. Chem. Ges.* **1896**, *29*, 1559.
(2) Angeli, A. *Chem. Zentralbl.* **1902**, *73* (II), 691.
(3) (a) Angeli, A. *Chem. Zentralbl.* **1896**, *67* (I), 799. (b) Angeli, A. *Gazz. Chim. Ital.* **1903**, *33* (II), 245.
(4) Smith, P. A. S.; Pars, H. G. *J. Org. Chem.* **1959**, *24*, 1325.
(5) (a) Hawthorne, M. F. *J. Am. Chem. Soc.* **1957**, *79*, 2510. (b) Hawthorne, M. F.; Strahn, R. D. *J. Am. Chem. Soc.* **1957**, *79*, 2515. (c) Ibid. **1957**, *79*, 3471.
(6) Corrie, J. E. T.; Kirby, G. W.; Laird, A. E.; MacKinnon, L. W.; Tyler, J. K. *J. Chem. Soc.* **1978**, 275.
(7) Jorgenson, K. A.; Shabana, R.; Scheibye, S.; Lowenson, S. O. *Bull. Soc. Chim. Belg.* **1980**, *89*, 247.

0020-1669/92/1331-2514$03.00/0